SECTION 3
PHYSICS OF RADIATION AND ION-PLASMA TECHNOLOGIES

https://doi.org/10.46813/2024-152-100

UDC 669.017:539.16

HYDROGEN BARRIER COATINGS AND THEIR PERMEATION RESISTANCE

G.D. Tolstolutska[1], M.O. Azarenkov[1], V.A. Bilous[1], O.S. Kuprin[1], M.G. Ishchenko[2]
[1]National Science Center "Kharkov Institute of Physics and Technology", Kharkiv, Ukraine;
[2]JSC "Ukrainian Energy Machines", Kharkiv, Ukraine
E-mail: g.d.t@kipt.kharkov.ua

This review discusses the state of the art in hydrogen permeation for a variety of coatings. Hydrogen ingress into structural materials can be detrimental due to corrosion and embrittlement. To enable safe operation in applications requiring protection from hydrogen isotopes, recent advances in material design and performance characterization of barrier coatings to prevent hydrogen isotope absorption ingress and permeation are summarized. Alternative coating concepts can provide greater resistance to hydrogen isotope permeation along with other improved properties such as mechanical strength and thermal resistance. The information presented here focuses on recent findings of promising hydrogen barriers including oxides, nitrides, carbon, carbide, MAX phases, and metals and their mechanical strength, hydrogen uptake, and radiation resistance.

INTRODUCTION

Hydrogen energy has been considered the most potential new energy to replace fossil fuels in the 21st century due to its natural abundance, large energy density (143 kJ/g), recyclability, and pollution-free combustion product (water) [1]. However, it is essential to resolve many technical problems in relation to hydrogen use. Specifically, advancements in fuel cell technology, hydrogen production and storage methodologies, and the development of materials and systems capable of enduring cyclic loads in a hydrogen-rich environment are imperative.

Synergic action of stress and environment may result in various types of degradation of metallic materials. There are the following several specific types of hydrogen-induced damage of metals and alloys: hydrogen embrittlement; cracking from precipitation of internal hydrogen; cracking from hydride formation; hydrogen attack; hydrogen-induced blistering [2].

One of the key challenges in the development of the hydrogen energy storage and transportation industries is the reduced lifetime of components used in the transmission and containment of hydrogen. This is due to the phenomenon of hydrogen embrittlement, which can cause significant damage to these components. As a result, mitigation of the damage caused by hydrogen embrittlement is crucial to ensuring the reliability and longevity of these components, and ultimately, the success of the hydrogen energy industry.

The embrittlement of a metal is caused by the diffusion of gaseous hydrogen within the material's structure. During the hydrogen diffusion, extreme stress and distortion of the metallic crystal lattice are created, which leads to a reduction of the toughness on the surface of metal materials up to cracking and ultimately results in the leakages of hydrogen and its isotopes, deuterium and tritium [3, 4]. Hydrogen embrittlement is an irreversible phenomenon that must be prevented, as once the damage to the structure occurs, it will be permanent, and it is impossible to do any treatment.

Fig. 1 illustrates the key mechanisms that exist to improve the hydrogen resistance in steel [2]. Barrier coatings for hydrogen-entry obstruction are one of the most promising technologies under investigation, with many studies on barrier coatings reported thus far [5, 6].

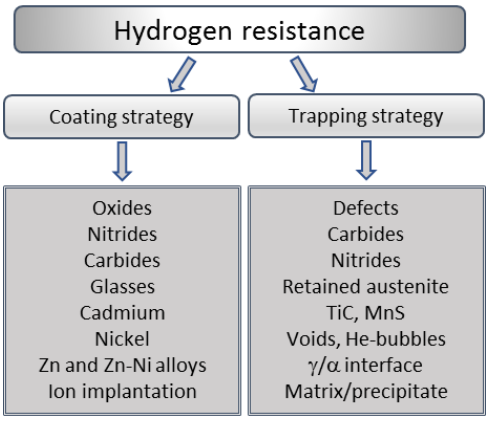

Fig. 1. Mechanisms available for the modification of steel for higher hydrogen resistance [2]

An abundance of coatings exists that to reduce either the outgassing of hydrogen in vacuum systems, or serve as diffusion barriers to the ingress of hydrogen. However, the choice of available coatings is reduced when the coating must perform multiple functions such as wear, abrasion and impact resistance. The thickness and integrity of the coating depends on the manufacturing process and must be compatible with the operating conditions of the protected component. The quality of the coating may depend on the chemical composition and structure of the substrate. In addition, ion implantation can be used to modify the steel surface.

However, the choice of coatings available decreases when the coating has to perform multiple functions, for example to resist abrasion and impact. The thickness

and integrity of the coating will vary with the manufacturing process and has to be compatible with the service conditions of the protected component. The quality of the coating can depend on the chemical composition and structure of the substrate. Ion implantation can be used to favorably alter the surface of the steel

Unfortunately, the most advanced coatings cannot prevent the accumulation of hydrogen in materials subjected to intense neutron irradiation, since in this case hydrogen is generated directly in the bulk of the material through transmutation reactions. In such a situation, in order to neutralize the harmful effect of hydrogen and increase the resistance of materials to hydrogen embrittlement, the concept of using hydrogen traps, which capable to reliably retain it the entire service lifetime in the whole operating temperature range of the nuclear facility, purchases the key importance.

Hydrogen barrier coatings comprise thin layers of materials that exhibit low inherent hydrogen permeability and solubility. These coatings have the potential to significantly slow down, reduce, or prevent hydrogen diffusion. By implementing these coatings, it is anticipated that steels prone to hydrogen embrittlement, particularly low-cost low-alloy and lightweight high-strength steels, can be utilized in various applications within a hydrogen economy [7].

Hydrogen barriers play a vital role in ensuring the safe development and operation of clean energy infrastructure, including fusion reactors and future Generation IV (Gen IV) nuclear reactors. Additionally, they are essential for containing spent fuel and mitigating risks associated with nuclear reactors. Some Gen IV reactors will be designed to produce hydrogen, while others will utilize high-temperature salt-coolants, making the development of robust hydrogen barriers crucial for their successful implementation. The implementation of an effective barrier is crucial for mitigating the risks associated with nuclear reactor incidents. By preventing material failures of tanks, structures, and pipelines, the likelihood of accidents can be significantly reduced or, at the very least, their severity minimized. Furthermore, the development of advanced materials can help to mitigate the consequences of exothermic reactions between Zirconium and water, as exemplified by the 2011 Fukushima Daiichi nuclear accident. This incident has subsequently spurred a surge in research focused on improving materials' performance and reliability in nuclear applications [8].

The uses of hydrogen barriers in materials is essential for ensuring a prolonged lifetime and mitigating the economic burden associated with frequent replacements of components due to hydrogen-induced embrittlement. In the context of nuclear applications, numerous hydrogen barriers have demonstrated exceptional resistance to permeation in controlled laboratory settings. However, a significant gap in performance is observed when these materials are deployed in a radiation environment, where their efficacy is compromised. The impact of irradiation and implantation on the transport of hydrogen isotopes in materials is a significant consideration. In addition to exhibiting resistance to hydrogen absorption and permeation, coatings must also possess reasonable ductility and strength to prevent cracking during fabrication and service [9].

The aim of this article is to review the status of barrier coatings, including oxides, nitrides, carbon, carbides, MAX phases and metals, and their resistance to hydrogen isotope permeation, to compare coating methods in terms of their ability to produce layers of suitable quality and their scaling potential for industrial use, and to consider, in addition to existing commercial coatings, alternative concepts that could provide greater resistance to hydrogen isotope permeation along with other improved properties such as mechanical strength and thermal stability.

1. MECHANISM FOR HYDROGEN PERMEATION

The permeation of hydrogen isotopes through solid materials is a well-established phenomenon that occurs through a multi-step process involving adsorption, dissociation, diffusion, and recombination, culminating in desorption. This process can be significantly hindered by the presence of an effective barrier that impedes the initial ingress of hydrogen isotopes into the film, thereby preventing their subsequent diffusion into the underlying substrate. Fig. 2 shows a schematic representation of hydrogen permeation in a coated sample, where the permeation process is assumed to proceed through the entire substrate and culminate in desorption and recombination, as previously reported [9].

The hydrogen molecule (H_2) is adsorbed on the surface of the film, subsequently undergoing dissociation into hydrogen atoms (H). The adsorbed hydrogen atoms undergo absorption, diffusing into the film from the surface and migrating towards the interface with the substrate. The hydrogen pick-up barrier is designed to prevent the diffusion of hydrogen atoms into the film and further into the substrate, thereby regulating the rate of hydrogen uptake.

However, hydrogen atoms can also diffuse from the interface of the film to the non-coated side of the substrate, where they recombine to form hydrogen molecules and subsequently undergo desorption.

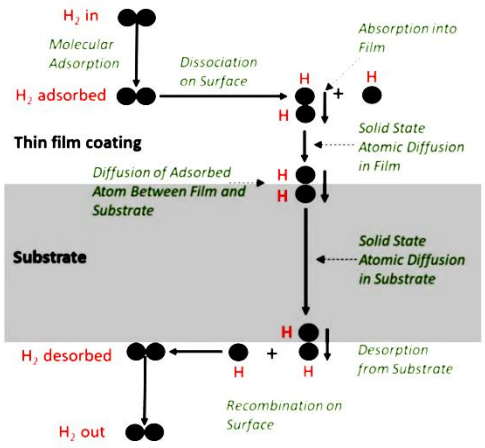

Fig. 2. Illustration of hydrogen permeation in a thin film coated substrate [9]

Permeability of hydrogen and its isotopes is the steady state diffusional transport of atoms through a material as illustrated in Fig. 2 that supports a differential pressure of the hydrogen isotope.

A large amount of data was obtained in studies of thermodynamic and kinetic features of the iron-hydrogen system [10–20]. At the same time, the data of various researchers often show discrepancies in solubility, and especially in the diffusion ability of hydrogen (Table 1). Several possible factors that lead to observed disagreements are considered. The most important are the following effects that lead to "distortion" in the measurements of solubility: 1) the interaction of hydrogen atoms with point defects (interstitial and vacancies) in a lattice of iron; 2) the influence of metallurgical factors, such as grain boundaries and impurities; 3) deformation-related defects, such as dislocations; 4) traps or contaminations on the material surface.

The diffusion of hydrogen in non-irradiated stainless steels practically does not depend on the composition of austenite. The hydrogen diffusivity in ferrite-martensitic steels is also slightly different from each other [2].

Table 1

Hydrogen solubility and diffusion coefficients (D) in iron and steels

Material	T, K	Solubility, N_H/N_{Fe}	$D = D_0 \exp(-E_m/kT)$, m^2/s	D (573 K), m^2/s
X18H10T	423…723	$10^{-4}…10^{-3}$	$D=8.4\cdot10^{-7}\exp(-0.58/kT)$	$6.5\cdot10^{-12}$
SS316	373…723	$10^{-4}…10^{-3}$	$D=6.2\cdot10^{-7}\exp(-0.535/kT)$	$1.19\cdot10^{-11}$
Fe	373…743	$10^{-8}…10^{-6}$	$D=6.7\cdot10^{-8}\exp(-0.087/kT)$	$1.15\cdot10^{-8}$
EUROFER	523…873	$10^{-6}…10^{-4}$	$D=1\cdot10^{-7}\exp(-0.14/kT)$	$5.84\cdot10^{-9}$

Low solubility (1...10^2 appm) and high diffusion mobility (10^{-11}...10^{-8} m^2/s) contribute to minimizing of hydrogen accumulation in iron and steels in the absence of microstructural defects. But the concentration of hydrogen that can cause the embrittlement of metals is also quite small (~ 1 wppm) (Fig. 3).

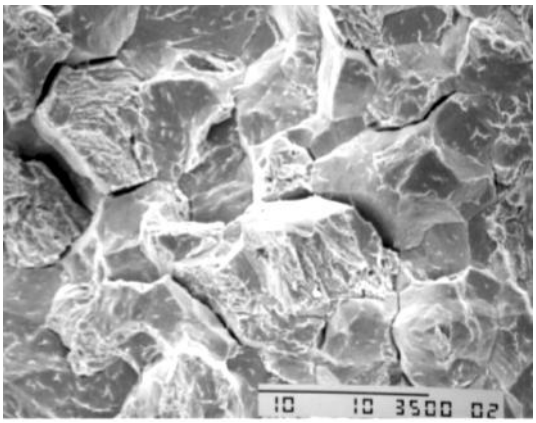

Fig. 3. SEM image of the fracture surface for F82H martensitic steel (0.61 wppm H content), showing typical intergranular H-fracture with several secondary cracks. The bar corresponds to 10 μm [20]

At the same time, it is extremely important to estimate the effect of impurities on the dissolution energy of hydrogen in a metal that affects the content of hydrogen. Such an estimate will allow the identification of impurities capable of hydrogen trapping and thereby preventing the formation of bubbles, that opens the way to controlling the solubility of hydrogen and to prevent negative impacts on the mechanical strength of materials.

A comprehensive review of various materials that exhibit effective hydrogen barriers has been conducted, revealing a range of commercially available options. The efficacy of these materials for a specific application is contingent upon a multitude of factors, including temperature, pressure, microstructure, coating thickness, compatibility with the substrate, and occasionally, compatibility with chemical reactions.

It is essential to carefully select a hydrogen permeation barrier that is tailored to the specific application, accompanied by a suitable manufacturing method. A comprehensive review of existing literature reveals that various classes of hydrogen permeation barriers have been investigated, including oxides, nitrides, carbides, carbon, metals, and intermetallic compounds [21].

2. COATING APPLICATION METHODS

A comprehensive review of the existing literature reveals the many techniques for the deposition of hydrogen permeation barriers, which can be classified into three primary categories: physical vapor deposition (PVD), chemical vapor deposition (CVD), and wet chemical deposition techniques. These categorizations are supported by references [7, 9], which provide a detailed overview of the various methods employed for the deposition of hydrogen permeation barriers.

The nomenclature PVD and CVD refers to two distinct categories of vacuum deposition techniques that involve the transfer of material from a source to a substrate. In PVD processes, the coating material is evaporated and subsequently condensed onto the substrate through a process of thermal or electron beam evaporation. Conversely, CVD techniques involve the chemical reaction or decomposition of a gaseous precursor at the substrate surface, resulting in the deposition of a thin film.

A prevailing methodology for the deposition of protective coatings on steel substrates is thermal spraying, which involves the application of various metallic materials such as aluminum, copper, tin, lead, nickel, zinc, and molybdenum. Despite its widespread adoption, thermal spraying typically yields a residual porosity of approximately 18%, rendering it a persistent challenge [22]. Moreover, ceramic coatings produced via thermal spraying often exhibit inhomogeneous

microstructures characterized by the presence of multiple crystalline and amorphous phases.

The sol-gel process has been employed for the deposition of non-metallic, inorganic materials such as alkoxides and halogenides. The cold spray technique is beneficial when it is necessary to avoid introduction of thermal stress that can occur at high temperatures. Other benefits include no "heat-affected zone" (HAZ) due to very low heat input. However, this method often yields nanoporous layers with insufficient compaction, which can compromise their structural integrity [22]. In contrast, metal-organic CVD (MOCVD) has emerged as a reliable technique for the synthesis of hydrogen-resistant coatings comprising dispersed ZrO_2, Al_2O_3, or Cr_2O_3 on the interior surfaces of pipes. These coatings, which range in thickness from 100 nm to 20 μm, have been shown to exhibit significantly improved hydrogen resistance under mild conditions, with a enhancement factor of 300 demonstrated in comparative studies [23].

Vacuum-based deposition processes, specifically PVD and CVD, exhibit excellent suitability for the fabrication of dense ceramic layers. However, industrial-scale vacuum-based processes often necessitate significant capital expenditures, potentially offsetting the benefits of these techniques. This disparity in investment requirements may pose a significant challenge for operators seeking to balance production costs with the quality of ceramic layers produced.

The drawback associated with this methodology is mitigated by a significant decrease in production costs when large quantities are produced. Through the employment of vacuum evaporation, it was possible to consistently synthesize homogeneous and dense Al_2O_3 layers, allowing for the successful coating of inner surfaces with diameters of 10 mm and lengths of 3.8 m [24]. Thermally emitted electrons were accelerated by an electric field and focused onto the coating material, thereby inducing melting and subsequent deposition onto the substrate [25]. A notable example of the efficacy of this technique is demonstrated by the deposition of 500 nm thick layers of Al_2O_3 onto an amorphous WO_3 substrate via electron beam evaporation [26]. The results indicate effectiveness of thin vapor deposited Al_2O_3 film as a permeation barrier against atomic hydrogen.

Brief summary of the advantages and disadvantages of each method is provided in Table 2, allowing for a comparative analysis of the strengths and limitations of each technique. This information will facilitate informed decision-making in the selection of the most suitable method for specific research applications [7].

Table 2

Advantages and disadvantages of the main deposition methods [7]

Method	Advantages	Disadvantages
Physical vapour deposition (PVD)	• High purity and density of deposited film • Low process temperature	• Limited large-scale applicability, small deposition chamber, and high capital and operating costs • Limited ability to enter pores
Chemical vapour deposition (CVD)	• Ability to enter pores and cover complex shapes • The process can be easily scaled up	• Deposition requires high temperatures and can be energy-intensive • High capital and maintenance cost
Galvanic deposition	• Suitable for coatings on complex shapes • Relatively low-cost method	• Relatively low effectiveness as a barrier coating • Possible hydrogen uptake during deposition
Hot-dipping	• Can cover complex shapes and enter pores. • Low cost and widely available	• Process may not be suitable for all types of substrates or coatings • Difficulty achieving a uniform coating over a large area
Thermal spraying	• Can produce durable coatings • High deposition rate	• Limited effectiveness as a barrier coating due to porosity • The process is energy-intensive • May produce inhomogeneous coatings with poor adhesion
Pack cementation	• The process can be easily scaled up for large-scale production • Low cost and widely available	• The process is slow and shows limited ability to enter pores • Limited durability and effectiveness of the coatings
Sol-gel	• The process is relatively low-cost • Can be easily scaled up for large-scale production	• Limited durability and effectiveness of the porous coatings • Difficulty achieving a uniform coating over a large area

To ensure the effective application of a coating on a specific substrate or cladding, a comprehensive characterization process is necessary. This includes evaluating the compatibility of the coating with the substrate/cladding, assessing the integrity of the materials in the applied environment, determining permeation resistance, and measuring mechanical strength. By conducting these characterizations, fabricators can guarantee the optimal performance and functionality of the coated material for its intended use.

To investigate the microstructure and surface chemistry of materials, researchers have access to a

range of advanced analytical tools, including scanning electron microscopy (SEM), transmission electron microscopy (TEM), atomic force microscopy (AFM), and X-ray photoelectron spectroscopy (XPS).

However, when a material is intended for use in nuclear reactors, additional testing is necessary to evaluate its performance and integrity under irradiation conditions. This involves exposing the material to controlled levels of radiation to simulate the conditions it will encounter in a nuclear reactor, allowing researchers to assess its response and potential degradation over time.

3. ADVANCES IN HYDROGEN BARRIER COATINGS

3.1. METALS

3.1.1. Chromium. Chromium coatings have been much investigated recently and is a leading candidate in the nuclear industry.

To date, in the literature there is no systematic data on the effect of irradiation dose and temperature on the same chromium coatings. However, it should be noted that during operations with fuel elements, their temperature can change. In this case, the coating material will be irradiated at different temperatures, and therefore, its structure stability under irradiation should be studied. The influence of 1.4 MeV argon ions irradiation to the doses of 5, 15, and 25 dpa within the temperature range of 300…550 °C on the swelling of chromium coatings deposited by the cathodic arc evaporation method was studied [27]. The increase in the irradiation temperature from 300 up to 550 °C induces the increase in the mean size of voids from 3 to 8.6 nm, thereby decreasing their concentration from $3 \cdot 10^{17}$ to $2.1 \cdot 10^{16}$ cm^{-3} (Fig. 4).

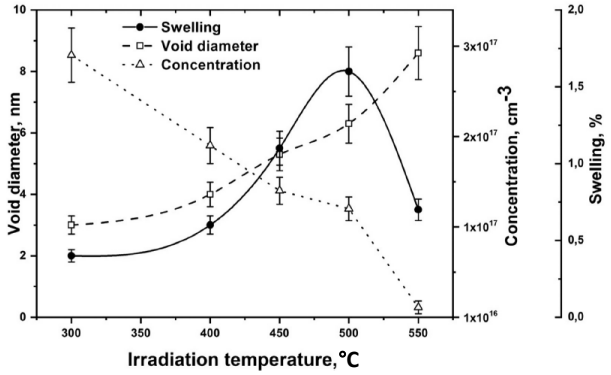

Fig. 4. The temperature dependence for the diameter, concentration of voids and swelling in the Cr coatings irradiated up to 25 dpa [27]

The radiation-induced swelling of 0.4% is observed at the temperature of 300 °C, and the maximum of 1.6% is reached at the temperature of 500 °C. This is more than twice lower than the allowable swelling for the reactor materials. So, chromium coatings have a good radiation resistance, and are therefore a good candidate for providing corrosion and oxidation protection of zirconium alloy claddings for PWR- and BWR-type reactors [27, 28].

3.1.2. Hydrogen solubility data of pure metals A review of hydrogen permeability data of solid metals in Table 3 shows that there are a few pure metals with very low permeability [29].

Table 3

Hydrogen permeability of metals at 400 and 500 °C [29]

Metal	*P*	*T*
	mol H_2/m/s/ $Pa^{0.5}$	°C
Vanadium	2.9×10^{-8}	500
Titanium	7.5×10^{-9}	500
Nickel	1.2×10^{-10}	500
Ferritic steels	3×10^{-11}	500
Austenitic steels	$0.9–1.2 \times 10^{-11}$	500
Molybdenum	1.2×10^{-11}	500
Tungsten	4.3×10^{-15}	500
Beryllium	2×10^{-15}	400

It should be noted that the diffusion process through solid metals, applied as a Hydrogen Permeation Barrier (HPB) efficiency, requires a complex description with some more parameters which can only be extracted from the transient phenomena in permeation rate experiments [30].

3.1.3. Multicomponent metallic coatings based on Cr, Ti, Al, Fe, Y, Si deposited by the cathodic arc evaporation method have been studied for the protection of Zr1Nb alloy fuel rod cladding [31]. Research samples of metallic coatings (Cr, TiAlCrY, FeCrNi) with a thickness of 5…9 μm on the cylindrical surface of fuel rod tubes were synthesized. The metallic coatings have a thin Cr sublayer. Fig. 5 shows the weight gain histograms of the samples after the high temperature oxidation test. All coated samples oxidize significantly less in air than uncoated Zr1Nb samples at all test temperatures, and this advantage increases with increasing temperature. The metallic coatings show the best resistance to high temperature corrosion. For example, the weight gain of Cr coated samples at 1100 °C is 6.3 times less than that of uncoated samples.

At an annealing temperature of 1100 °C, the uncoated sample oxidizes to a depth of 130 μm within one hour to form crystalline ZrO_2 oxide, while in the coated samples, oxygen penetrates only to the surface layer, forming a thin oxide film that prevents further oxidation. The depth of oxygen penetration does not exceed 3…5 μm. The phase composition of the subsurface layer of the coating does not change significantly.

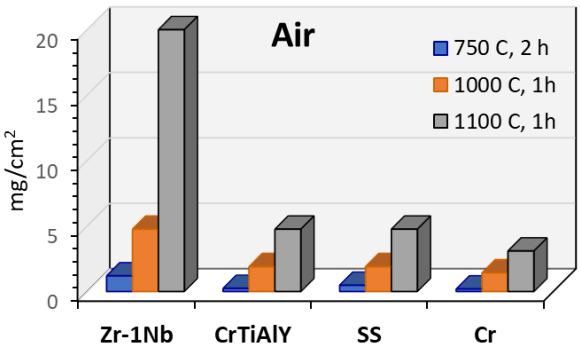

Fig. 5. Weight gain of samples after oxidation in air after thermocycling (3 times for 20 min) in a steam at 1020 °C (only the top layer of the coating is shown)

The use of metallic coatings to protect the Zr1Nb alloy surface from oxidation during thermal cycling in water vapor is also effective (Fig. 6).

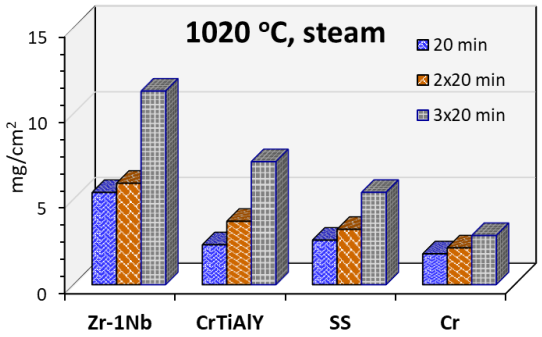

Fig. 6. Weight gain of samples after thermocycling (3 times for 20 min) in a steam at 1020 °C (only the top layer of the coating is shown) [31]

The Cr coating oxidizes only up to 3 μm. The Cr/SS and Cr/TiAlCrY metal coatings allow oxygen to penetrate three times deeper, but prevent oxidation of the zirconium alloy.

Chromium-based metal coatings have shown the best protective properties in simulated accident tests. They are also resistant to high-temperature corrosion in air and steam during thermal cycling.

As demonstrated in [32], cold spray Cr coatings exhibit superior high-temperature oxidation resistance compared to Zr-4 alloy. The coating exhibits greater nonuniformity compared to PVD, yet cold spray boasts a high deposition rate and is well-suited for industrial production. The samples were subjected to oxidation in high-temperature steam at 1200 °C and demonstrated effective prevention of oxidation.

3.1.4. FeCrAl coatings. The FeCrAl alloy system has been extensively researched for 50 years, with a focus on its potential applications in the nuclear industry. It has been investigated as a cladding material due to its excellent thermal and mechanical properties, including high melting points, strength-to-weight ratios, and resistance to corrosion and oxidation. Additionally, it has been found to have low thermal conductivity, which is desirable for minimizing heat transfer between fuel and coolant. It has also been investigated as a HPB in nuclear reactors, preventing the diffusion of hydrogen from coolant into the reactor core. This is important in light water reactors where hydrogen production can pose safety concerns. The continued research of FeCrAl alloys is expected to lead to significant advances in reactor design and operation, improving safety, efficiency, and sustainability in the nuclear energy sector.

A comprehensive investigation was conducted to examine the permeation of hydrogen and tritium in various FeCrAl alloys at temperatures ranging from 200 to 700 °C. The purpose of this study was to determine the permeability of these alloys and identify potential mitigation strategies. The results indicated that FeCrAl alloys with higher chromium (Cr) content exhibited lower permeability compared to those with lower Cr content [33].

Notably, a substantial disparity in permeability exists between specimens that have undergone oxidation and those that have not. Specifically, the presence of an alumina (Al_2O_3) layer on oxidized specimens has been demonstrated to result in a nearly one-order-of-magnitude reduction in permeability relative to the typical values observed for bare FeCrAl alloys

The specific features of the process of saturation of coatings made of FeCrAl alloy and Kh18N10T stainless steel with deuterium from gaseous atmospheres were studied [34]. The influence of the surface morphology and chemical compositions of the coatings on these processes was revealed. The obtained results were compared with the level of accumulation of deuterium in the Zr1Nb alloy saturated under the same conditions. It was demonstrated that the quantity of deuterium accumulated in the coatings is considerably less than that observed in the zirconium alloy (~ 0.014…0.003 and 0.1 at.%, respectively). The lowest retained deuterium concentration was observed in steel coatings deposited in an oxygen-rich atmosphere (~ 0.003 at.%), whereas the highest concentration (~ 0.014 at.%) was observed in coatings deposited in nitrogen (Fig. 7).

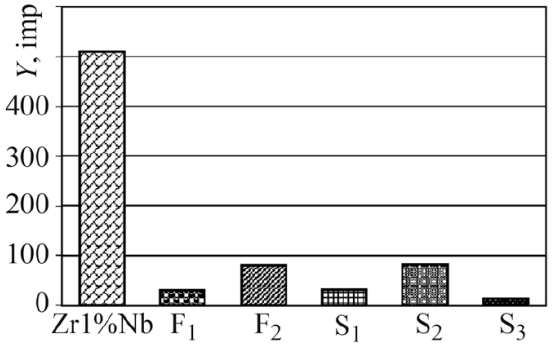

Fig. 7. Integral proton yields (Y, imp) for Zr1Nb samples and coatings of FeCrAl alloy (F1 and F2) or Kh18N10T stainless steel (S1, S2, and S3) saturated with deuterium in vacuum (subscript 1), nitrogen (subscript 2), or oxygen (subscript 3) [34]

We found no difference between the amounts of deuterium retained in FeCrAl and Kh18N10T. Deuterium does not penetrate into the bulk of the coatings and is adsorbed in their subsurface zones, from which it is desorbed at a heating temperature higher than room temperature by 20…30 °C. Thus, we have demonstrated the prospects of application of vacuum arc coatings based on FeCrAl alloys and Kh18N10T stainless steel for the purposes of protection of zirconium alloys against saturation with hydrogen and its isotopes.

3.2. NITRIDES

A significant body of research has demonstrated the efficacy of nitride-based thin films in mitigating hydrogen uptake. Specifically, binary nitrides comprising chromium (CrN) and zirconium (ZrN) have been widely employed as coatings on stainless steels in industrial applications. Furthermore, titanium nitride (TiN) and chromium nitride (CrN) have recently garnered substantial attention in the nuclear industry for their potential to prevent corrosion and impede hydrogen ingress and diffusion into cladding and structural materials. Several groups are working to improve properties for specific applications by using

alloying additives, multilayering, and different manufacturing methods to alter microstructural features.

3.2.1. Chromium Nitride. Chromium nitride (CrN) has been employed as a corrosion barrier in commercial applications on stainless steel substrates [35]. A recent investigation has reported on the deposition of commercially available thin films comprising CrN, TiAlN, and AlCrN using PVD techniques, resulting in coatings with thicknesses ranging from 2…4 μm on Zircaloy-4 substrates [36]. This study investigated the corrosion resistance and impact on hydrogen permeability of various coatings. The corrosion resistance was evaluated under controlled conditions, including immersion in distilled water at 350 °C for a period of 24 h and exposure to simulated CANDU conditions (300 °C, pH 10.5) for 30 days. The results indicate that the CrN-coated samples demonstrated superior corrosion resistance compared to other coatings under pressurized water reactor, CANDU, and superheated steam conditions. Furthermore, the oxidation of both CrN and TiAlN coatings was found to significantly reduce hydrogen uptake.

The theoretical analysis revealed that the majority of CrN surfaces are inert to hydrogen and do not adsorb it [37]. To substantiate these findings, CrN coatings were produced using the Pulsed-DC magnetron sputtering method on gadolinium substrates. The coated samples were subsequently exposed to hydrogen and demonstrated that the coated samples exhibited no hydrogen-induced damage, whereas the uncoated samples displayed a significant degree of hydrogen attack [37].

The CrN coating deposited by arc ion plating was found to suppress hydrogen permeation into the aluminum alloy [38].

Depth distribution profiles of deuterium in zirconium alloy Zr1Nb in the initial state and with coatings CrN, CrAl and alumina after saturation in gaseous phase at temperature 300...600 °C (P_{D2} = (2…9)·10^{-3} Pa, time – 120 min) are determined by the method of nuclear reactions [38]. Fig. 8 shows histograms of the energy dependence of the integral proton yield obtained during the analysis of Zr1Nb samples without and with coatings of different composition.

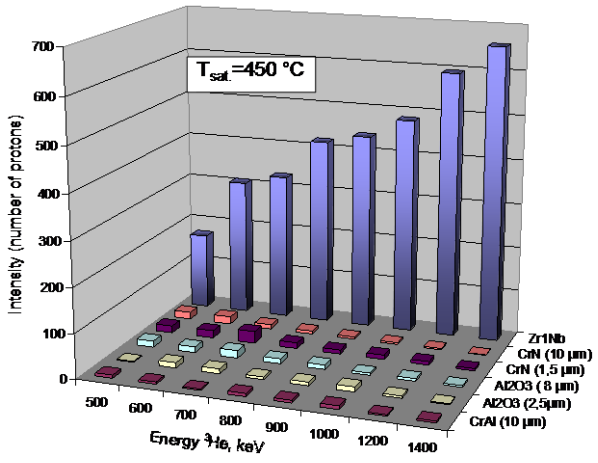

Fig. 8. Energetic dependences of the integral yields of protons for Zr1Nb samples with and without coatings saturated with deuterium at 450 °C [39]

Comparison of the data represented on histograms (see Fig. 8) shows that in the whole range of energies of the analyzing beam the integral yield of protons for the deuterium-saturated alloy Zr1Nb without coatings at 450 °C is two and at T_{sat} = 550 °C (see [39]) even three orders higher than for Zr1Nb with coatings.

Thus, chromium nitride PVD coatings can serve as a reasonably effective barrier with high mechanical properties against hydrogen and its isotopes permeation.

3.2.2. Titanium Nitride. Titanium nitride has been suggested as an exceptional hydrogen barrier material due to its remarkable properties, including a high melting point, exceptional hardness, excellent resistance to ion irradiation damage, and high thermal conductivity. Recent research has yielded encouraging advancements in the development of materials designed to mitigate corrosion and hydrogen uptake, thereby enhancing their durability and longevity. Notwithstanding these promising findings, supplementary investigations are warranted to comprehensively elucidate the behavior of hydrogen permeation in these materials, with a view to optimizing their performance and broadening their practical applications.

Researchers studied the properties of titanium nitride (TiN) coatings on stainless steel, finding that they reduce hydrogen permeation by 100–5000 times compared to uncoated steel. The size of the TiN grains affects the permeability, with larger grains allowing more hydrogen to pass through. This research has implications for developing materials for hydrogen storage and transportation, as controlling grain size and structure could improve their performance [40–42].

In an effort to design and develop accident tolerant fuels (ATFs) with improved corrosion resistance, the performance of multilayered ceramic coatings was investigated [42]. A study revealed that the deposition of $Ti_{1-x}Al_xN$ (where x ranges from 0.54 to 0.67) and TiN coatings onto ZIRLO substrates via cathodic arc PVD (CA-PVD) effectively enhances the corrosion resistance of the resulting surface.

NSC KIPT has developed a series of processes for cathodic arc deposition of multi-component coatings based on chromium, titanium, aluminum, iron, yttrium, silicon, and their nitrides. These coatings are utilized to protect the shells of Zr1Nb alloy fuel rods. The applied deposition processes ensure the formation of coatings with a thickness of 5…9 μm on the cylindrical surface of fuel rod tubes, which have a homogeneous, dense structure and high adhesion to the substrate. Research samples of nitride coatings (TiAlN, TiAlYN, TiAlSiN, TiAlCrYN) have been synthesized (Fig. 9) [31].

The nitride coatings have a double Cr/CrN sublayer to improve adhesion. The composition, structure, mechanical properties and high temperature oxidation resistance of the samples were investigated. Fig. 9 shows the weight gain histograms of the samples after the high temperature oxidation test. All coated samples oxidize significantly less in air than uncoated Zr1Nb samples at all test temperatures, and this advantage increases with increasing temperature.

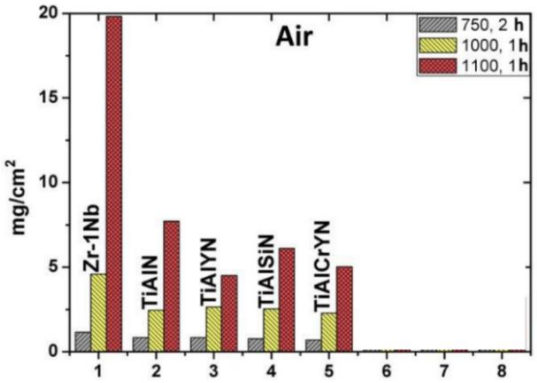

Fig. 9. Weight gain of samples after oxidation in air at 750 (2 h), 1020 (1 h), 1100 °C (1 h) (only the top layer of the coating is indicated) [31]

The use of coatings to protect the surface of Zr1Nb alloy from oxidation during thermal cycling in water vapor is less effective. Thermal cycling tests at 1020 °C with three thermal shocks of 20 min each showed that nitride-based coatings in most cases have almost the same weight gain as the Zr1Nb alloy (Fig. 10).

The reason for this is most likely that cracks have formed in the nitride coatings and oxygen has penetrated underneath. The thickness of the oxidized layer in the samples with nitride coatings ranges from 30 to 100 μm, while in the Zr1Nb sample without coating it is about 45 μm.

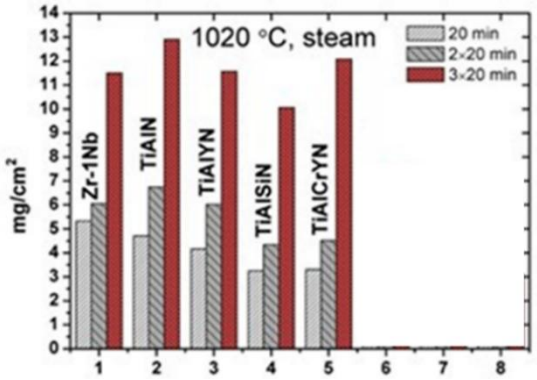

Fig. 10. Weight gain of samples after oxidation in a steam at 1020 °C (only the top layer of the coating is indicated) [31]

The hydrogen permeabilities of TiAlN-coated, TiN-coated, and TiAlN/TiMoN multilayer-coated samples were assessed at 573 K, revealing values of 1/100, <1/100, and <1/1000, respectively, relative to the uncoated 316L stainless steel substrate. These findings indicate that the newly developed multilayer coating exhibits a HPB performance 10 times superior to that of both TiN and TiAlN coatings, as depicted in Fig. 11 [43].

The TiC, TiN, TiAlN, and multi-layer TiAlN/TiMoN coatings were dense and showed excellent adhesion to the AISI 316 L austenitic stainless steel substrate. The hydrogen permeability of all coated samples decreased compared to that of the substrate alone, confirming the effectiveness of the coatings as hydrogen barriers.

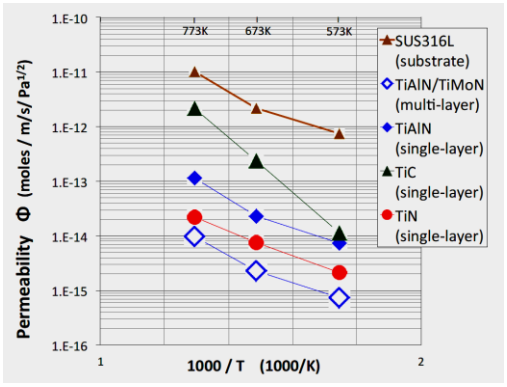

Fig. 11. The hydrogen permeabilities of coating TiC, TiN, TiAlN, and multi-layered TiAlN/TiMoN and AISI 316 L austenitic stainless steel [43]

3.2.3. Less Frequently Studied Nitrides. A comparative investigation was conducted to assess the HPB properties of less frequently explored nitride coatings, specifically AlCrN, Cr_2N, CrWN, WN, and ZrN, deposited via PVD [44]. The permeation reduction factor was evaluated for each coating material, yielding a range of approximately 10^2 to $5 \cdot 10^3$. Notably, the ZrN coating exhibited the most outstanding PRF performance among the examined materials.

Two distinct hydriding processes were successfully employed to produce zirconium hydride-impregnated samples of uncoated and coated Zircaloy-4 alloys. The electrochemical and gaseous hydriding methods yielded samples with homogeneous distributions of zirconium hydrides, as reported in [45]. Furthermore, ZrN thin films were deposited on the Zircaloy-4 substrate via the HCD-IP (a hollow cathode discharge ion-plating system). Following film deposition, the samples underwent separate treatments involving either electrochemical or gaseous hydriding. Fig. 12 illustrates the optical microscope (OM) observations of cross-sections after selective etching of zirconium hydride in samples with and without ZrN coating, subjected to two different hydriding methods.

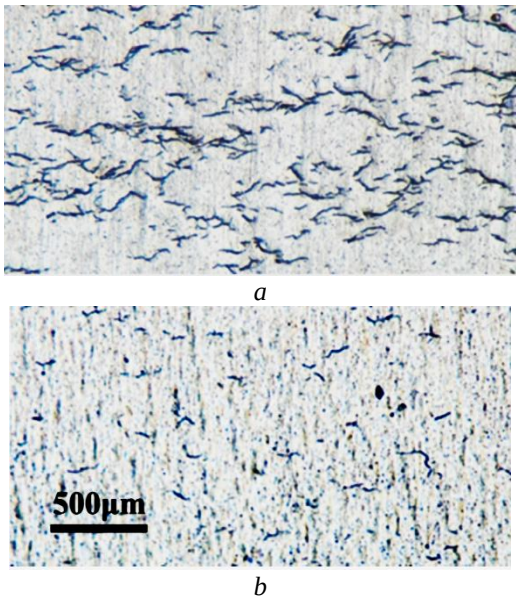

a

b

Fig. 12. The OM images over the cross-section of hydrided samples after selective etching [45]

According to the results of hydrogen analysis, the Zircaloy-4 samples without coating subjected to electrochemical and gaseous hydriding showed a reduction in hydrogen content of 82 and 89%, respectively. The results demonstrate that the ZrN thin films deposited by HCD-IP system exhibit significant resistance to hydrogen permeation, serving as effective hydrogen diffusion barrier layer.

As an important issue for ITER and DEMO, fuel retention and diffusion in first wall materials is a safety (tritium amount in ITER < 700 g [46]) and cost concern. In general, hydrogen retention in W is low, but diffusion is relatively fast at elevated temperatures (> 130 °C) [47].

The processes of deuterium retention of tungsten coatings have been studied under the influence of low energy (500 eV) deuterium plasma with fluence ($2 \cdot 10^{24}$ D^+/m^2) at room temperature [48]. The cathodic arc evaporation (CAE) method was used to deposit W and WN coatings on stainless steel substrate (Fig. 13).

The surface and the interface between the coating and the substrate are indicated by the white horizontal line. The coating thickness is approximately 5 μm. Within the coating we can see the grains with dimensions in the μm range and the absence of a pronounced columnar structure. Absence of columnar structure in these coatings can be explained by the sufficiently high energy of the deposited tungsten ions and the high degree of plasma ionization relative to the flow of evaporated material, which is characteristic of the cathodic arc evaporation method [49]. The WN coating has a near stoichiometric concentration of N ~ 50 at.% according to EDS analysis.

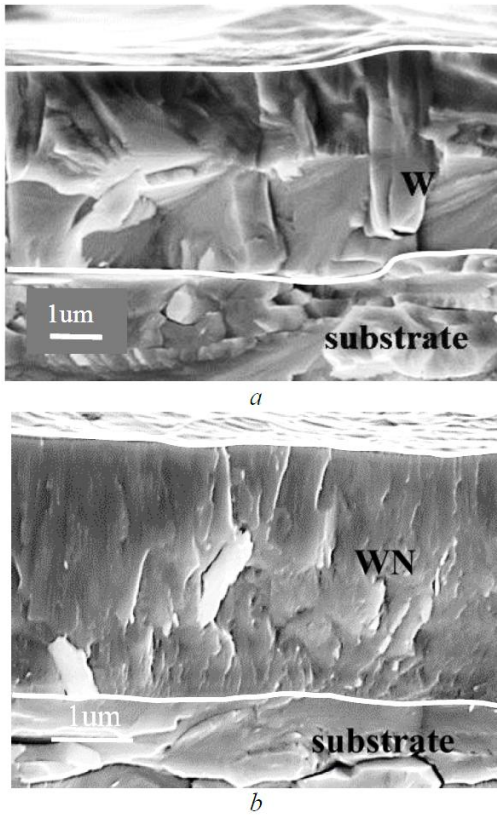

Fig. 13. Cross-section SEM images of W (a) and WN (b) coatings [48]

The retention and depth distribution of D in coatings after plasma exposure were measured by Nuclear Reaction Analysis (NRA) method [48]. Fig. 14 presents the depth distribution profile of deuterium implanted to a dose of $1 \cdot 10^{24}$ D_2^+/m_2 at T_{room} in W coating, and its evolution during aging at T_{room} for 30 days.

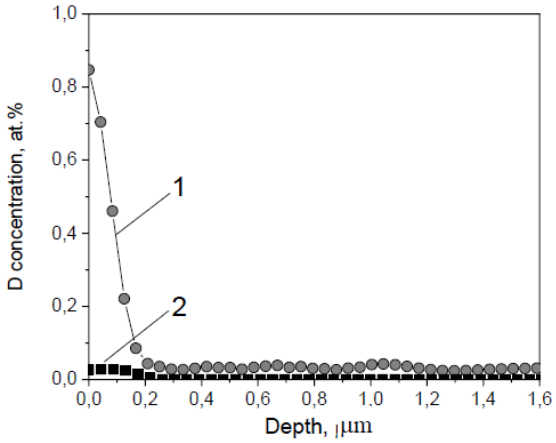

Fig. 14. Depth profiles of D in W coatings after the D plasma exposure (1) and after 30 days (2) [48]

NRA depth profiling of D-implanted WN films has indicated that D is retained only in a thin surface layer (< 0.2 μm) and even after exposure at T_{room} for 30 days (Fig. 15). However, its amount is decreased almost 1.5 times, probably due to desorption from the sample [50].

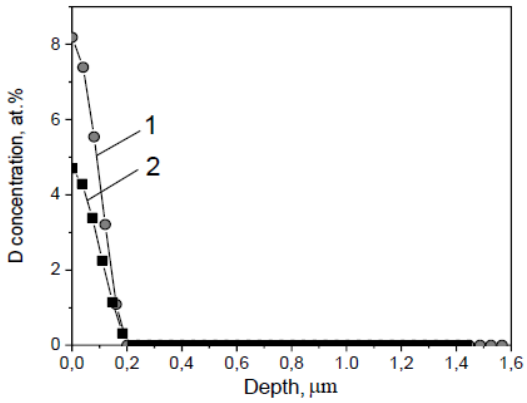

Fig. 15. Depth profiles of D in WN coatings after the D plasma exposure (1) and after 30 days (2) [48]

Thus, the permeation rates of deuterium through W coatings were observed to be approximately one order of magnitude higher than those of WN coatings, even at room temperature.

A comprehensive investigation was conducted on the deuterium permeation properties of tungsten (W), tungsten nitride (WN), and WN+W layers deposited onto Eurofer97 steel substrates [51]. The results of the experiments revealed a permeation rate factor (PRF) of 8 for pure tungsten, 31 for tungsten nitride, and 1000 for the WN+W multilayer structure at a temperature of 400 °C. It is noteworthy that the thermal expansion coefficient of tungsten differs significantly from that of martensitic steels, leading to the formation of cracks in tungsten coatings during thermal annealing, thereby precluding its use as a transition zone between the plasma-facing component and steel. In contrast, both

WN and WN+W coatings exhibited excellent thermal stability, remaining crack-free and thus suitable for application as transition zones on steel substrates.

A thorough examination of the permeation of hydrogen along grain boundaries in nanostructured tungsten thin films deposited on a nickel substrate was conducted in a recent study [52]. The investigation involved the performance of permeation measurements at temperatures ranging from 247 to 432 °C, yielding a consistently observed permeability ratio of approximately 4 across all temperature intervals.

The permeation of hydrogen along grain boundaries in nanostructured tungsten deposited on a nickel substrate was investigated [52]. Permeation measurements were conducted at temperatures ranging from 247 to 432 °C, yielding a consistent permeability ratio of approximately 4 at all temperatures.

Notably, the obtained permeability is significantly higher than that reported in the literature for specimens with larger grain sizes. The researchers attributed this enhanced permeability to the unique orientation of the grain boundaries relative to the surface. Specifically, they proposed that the perpendicular orientation of the grain boundaries facilitates hydrogen migration, leading to increased permeability.

3.2.4. Irradiation Experiments on Nitrides. Coatings of CrN, TiAlN, and AlCrN deposited on Zircaloy cladding in the Halden Reactor was conducted [53]. The investigation revealed that TiAlN and AlCrN coatings exhibited degradation under irradiation conditions, whereas the CrN coating demonstrated chemical stability in both Boiling Water Reactor (BWR) and Pressurized Water Reactor (PWR) environments. The disappearance of TiAlN and AlCrN coatings is likely attributed to the rapid dissolution of the aluminum oxide (Al_2O_3) that forms on the surface of these materials in both BWR and PWR water environments. Moreover, there was no reduction in coating thickness and CrN coatings reduce hydrogen uptake in zircaloy. Despite accident like conditions, most of the CrN coating was still intact after 150 days. When a crack occurs, oxide forms underneath and the expansion led to further cracking. CrN appears to be a viable hydrogen barrier for use in nuclear reactors [53].

Recent research has underscored the significance of **structural modification** as a viable means of enhancing the radiation tolerance of transition metal nitride coatings. In recent years, a many of structural modification methods have been proposed and investigated with the aim of improving the irradiation tolerance of these coatings. Within the realm of coating design, two prevailing structural strategies have garnered significant research attention: ***multilayer and compositional gradient approaches***. The multilayered architecture involves the assembly of distinct sublayer materials, thereby introducing numerous interfacial regions that serve as sinks for absorbing and/or dispersing radiation-induced defects. This design configuration frequently exhibits superior radiation resistance and mechanical properties compared to monolithic coatings.

A gradual variation in composition along the thickness direction of the coating is observed, leading to a continuous alteration of microstructure and chemical composition, thereby eliminating the presence of interfacial boundaries. This compositionally graded coating exhibit's superior mechanical reliability, characterized by high adhesion strength and thermal shock resistance. Furthermore, it was proposed that a hybrid coating system combining multilayered and compositionally graded structures represents a novel direction for enhancing irradiation resistance. This innovative approach leverages the benefits of both architectures to create a more resilient and robust coating system [9].

3.3. OXIDES

Over the years, various oxide coatings have been researched, including alumina (Al_2O_3), chromia (Cr_2O_3), erbia (Er_2O_3), and zirconia (ZrO_2). Recently, there has been a growing emphasis on nano-engineering oxides to enhance their properties. In addition, other approaches to materials engineering involve structural modifications and the use of dopants and mixtures.

3.3.1. Aluminum Oxide. Aluminum oxide, specifically Al_2O_3 (also known as alumina), has been chosen for its ability to act as a HPB on stainless steel and is utilized in a range of applications. Notably, alumina can exist in multiple metastable polymorphs, in addition to its thermodynamically stable α-Al_2O_3 form, which is also known as corundum [54].

Commercially available corundum, specifically in its alpha phase, is renowned for its exceptional HPB properties, boasting a PRF of over 1000…10,000 [55, 56]. While it excels in this regard, it still requires improvement in terms of mechanical and thermal strength. Moreover, when exposed to irradiation in a nuclear reactor, the coating's integrity is compromised. It's worth noting that other crystal structures of alumina do not possess the same level of hydrogen barrier effectiveness as the alpha phase.

Fig. 16 shows hydrogen contents of cylindrical specimens prepared from Type 304 austenitic stainless steel and exposed to high-pressure hydrogen gas at 100 MPa and temperature of 270 °C for 200 h.

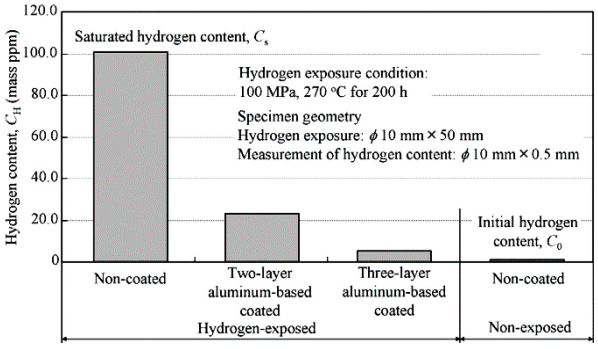

Fig. 16. Hydrogen contents of non-coated, two-layer aluminum-based coated and three-layer aluminum-based coated specimens exposed to hydrogen gas at pressures of 100 MPa, and temperature of 270 °C for 200 h measured by thermal desorption analysis [5]

The hydrogen content of the non-coated hydrogen-exposed specimen was 100.6 mass ppm, while that of the hydrogen-exposed specimen coated with the two-layer aluminum-based coating was 23.1 mass ppm. In

contrast, the hydrogen content of the hydrogen-exposed specimen with the three-layer aluminum-based coating was 5.0 mass ppm [5].

The results of experiments [57–60] suggest the potential for nanoceramic coatings beyond alumina to provide superior corrosion and wear resistance in high-radiation applications, including accident-tolerant fuels, Generation IV fuel cladding, and fusion tokamak tritium breeding components.

3.3.2. Zirconium Oxide. Zirconium oxide has been demonstrated to serve as a reliable hydrogen permeation barrier, wherein the formation of a zirconium oxide layer on the surface of zirconium or its alloys occurs naturally through corrosion in aqueous environments or intentionally via heat-induced oxidation. Notably, this property has been primarily explored in the context of nuclear applications, where the mitigation of hydrogen embrittlement and subsequent failure of zirconium-based materials is a critical concern [61]. Notably, zirconium oxide and yttria-stabilized zirconia (YSZ) have been investigated for their potential applications as hydrogen permeation barriers, in addition to their utilization as a debris-resistant feature at the bottom of some fuel rods [62].

In an effort to diminish the ingress of hydrogen into the alloy via the barrier oxide, two design strategies have been put forth in the literature [63]. The first approach involves incorporating a dopant, such as chromium (Cr), which decreases the solubility of hydrogen within the oxide. This reduction in solubility diminishes the likelihood of hydrogen entering the alloy through the oxide layer. Conversely, an alternative strategy entails incorporating a dopant, including niobium (Nb), tantalum (Ta), tungsten (W), phosphorus (P), and molybdenum (Mo), which accelerates the evolution of hydrogen at the oxide surface. This increased rate of hydrogen evolution facilitates the removal of hydrogen from the oxide layer, thereby minimizing its diffusion into the alloy.

The formation of tetragonal ZrO_2 layers with a thickness of approximately 180 nm on ferritic steel substrates was achieved through the utilization of dip coating and electrolytic deposition techniques [64]. The selection of these preparation methods was motivated by their potential for scalability, allowing for the deposition of thin films onto larger structures.

An investigation of hydrogen permeation was conducted at a range of temperatures (300…550 °C) and compared to a thinner counterpart (100 nm). Notably, the permeation reduction factor for the thicker layer exhibited an order of magnitude greater value (approximately 1000). This enhanced performance can be attributed to the reduced defect density in the thicker coating, thereby resulting in a decreased permeation rate.

3.3.3. Aluminide + Alumina; FeAl-Al_2O_3. Iron aluminides possess exceptional oxidation resistance, are cost-effective to produce, exhibit low density, offer impressive strength-to-weight ratios, demonstrate good wear resistance, and can be easily fabricated, making them a promising substitute for stainless steel in industrial applications due to their numerous advantages.

Aluminum oxide (Al_2O_3) is being researched as a potential material for tritium permeation barriers due to its superior properties. These properties include high melting point, chemical stability, low hydrogen solubility, and low permeability. This makes it suitable for containing tritium, a highly reactive gas with important implications for nuclear fusion and waste management. The material can withstand extreme temperatures without degrading, won't react with its environment, and restricts the passage of hydrogen isotopes like tritium. Its low permeability makes it an attractive candidate for applications where minimizing gas diffusion is crucial.

However, the disparity in thermal expansion coefficients between the metal substrate and oxide ceramic coatings induces a significant thermal mismatch, leading to coating failure in applications characterized by extreme temperature fluctuations. To mitigate this issue, a functional gradient transition layer is often employed to bridge the substrate-coating interface, as exemplified by the Fe-Al layer. This approach enables the accommodation of thermal stresses and strain through the gradual variation of material properties, thereby enhancing the overall durability and reliability of the coated system.

The formation of an aluminide coating typically entails a two-step process comprising aluminization and oxidation. Initially, interdiffusion occurs between Al atoms and Fe atoms on the substrate surface, yielding the formation of a (Fe, Al) solid solution or an Fe-Al intermetallic transition layer during the aluminization step. In the oxidation process, the aluminide layer undergoes selective oxidation, yielding a thin film of aluminum oxide (Al_2O_3). The formation of this aluminide coating can be accomplished through various deposition techniques, including PVD, CVD, hot-dipping aluminization (HDA), electrochemical deposition (ECD), packing cementation (PC), plasma sputtering (PS), and sol-gel processing [65].

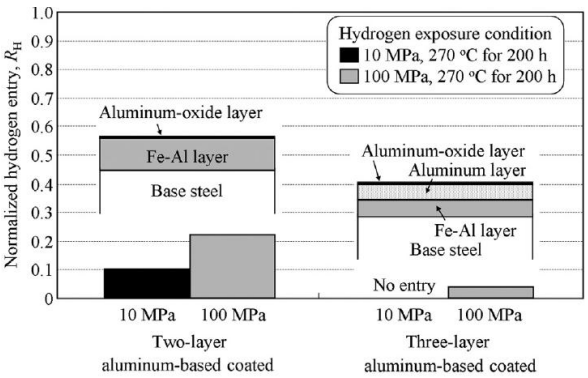

Fig. 17. Normalized hydrogen entry (RH) of two-layer aluminum-based coated and three-layer aluminum-based coated specimens exposed to high-pressure hydrogen gas at pressures of 10 and 100 MPa, and temperature of 270 °C for 200 h [5]

Fig. 17 shows the hydrogen-entry coefficient (R_H), of the two-layer and three-layer aluminum-based coated specimens exposed to hydrogen gas at pressures of 10 and 100 MPa at a temperature of 270 °C for 200 h. The R_H values of the two-layer aluminum-based coated

specimens were 0.10 at 10 MPa and 0.22 at 100 MPa [5].

A comparative analysis of hydrogen contents between specimens with two-layer and three-layer aluminum-based coatings, subjected to hydrogen gas pressures of 10 and 100 MPa, revealed that the three-layer coating exhibited an exceptional resistance to hydrogen entry.

It was shown that the tritium permeability of an γ-Al_2O_3/FeAl coated container of 321 stainless steel was reduced at 500…700 °C relative to a non-coated container [66], thus the permeation reduction factor was in the order of 1000…6000. the deuterium permeation depends on the steel substrate composition and microstructure [67].

The incorporation of alloying elements into the composition of TPB coatings enables the manipulation of their structural and performance characteristics. Notably, increases in carbon and aluminum content have been observed to reduce hydrogen diffusivity, resulting in decreased hydrogen diffusivity (increased PRF) [68]. Currently, research has primarily focused on the investigation of rare earth elements, including yttrium (Y), cerium (Ce), and hafnium (Hf), as beneficial alloying elements in aluminide coatings. These additives have been shown to enhance the wear, high-temperature oxidation, and corrosion resistance of aluminide coatings [65].

3.3.4. Bipolar Oxide: Chromium Oxide-Aluminum Oxide. The Cr_2O_3/Al_2O_3 bipolar oxide exhibits enhanced thermal stability compared to the Al_2O_3/stainless steel configuration, thereby promoting the formation of the thermodynamically stable α-Al_2O_3 phase [69]. The bipolar oxide was synthesized through a two-step process, involving electroplating of chromium onto 316L stainless steel to form a Cr_2O_3 film, which was subsequently oxidized to achieve the desired structure. Following the initial deposition of high-purity aluminum (Al) onto a chromium oxide (Cr_2O_3) film, the samples were subjected to oxidation and subsequent annealing procedures. The resulting bipolar oxides exhibited a combination of P-type semiconducting properties inherent to Cr_2O_3 and N-type properties characteristic of Al_2O_3. Notably, these bipolar oxides demonstrated superior hydrogen permeation resistance compared to individual coatings of Cr_2O_3 or Al_2O_3, highlighting the benefits of heterostructure formation in enhancing the material's performance.

3.3.5. Rare-Earth Oxides. A significant body of research has investigated the utilization of rare earth oxides for hydrogen barrier applications, owing to their exceptional thermal and mechanical stability in reducing atmospheres. A recent study examined the application of Er_2O_3 coatings on stainless steel substrates via the sol-gel method. The findings indicated that nanocrystalline Er_2O_3 coatings demonstrated remarkable efficacy in preventing the permeation of hydrogen isotopes, with a PRF of 300 [70]. Epitaxial Er_2O_3 thin films with exceptional quality were fabricated using ion beam sputter deposition onto a Si(100) substrate [71]. These films exhibited a remarkably low permeability of $4 \cdot 10^{-22}$ mol·$Pa^{-1/2}$·m^{-1}·s^{-1} at 873 K, which represents a significant improvement over Er_2O_3 coatings produced by alternative methods. Despite the outstanding properties of these films, several Er isotopes possess relatively high neutron absorption cross-sections, thereby limiting their potential application in nuclear reactors.

3.4. CARBON MATERIALS

Carbon-based materials have been extensively investigated for their potential as hydrogen storage media, encompassing a temperature range from room temperature to liquid nitrogen temperatures, as well as high-temperature applications within the realm of nuclear energy. Notably, graphite has been utilized as a structural and moderating material in nuclear power reactors and is being considered for deployment in next-generation nuclear reactors due to its unique properties. Recent research has explored the potential of carbon-based materials for hydrogen storage at extremely low temperatures. Specifically, carbides have been investigated for their capacity to serve as hydrogen barriers, while newer forms of carbon, including diamond-like carbon (DLC), graphene, metal-graphene hybrids, and graphene oxide, have been proposed as alternative hydrogen storage materials [9].

3.4.1. Diamond-Like Carbon (DLC). DLC coatings are a type of amorphous film composed of a mixture of diamond-like (sp3) and graphite-like (sp2) structures. These coatings exhibit exceptional properties, including high hardness, resistance to abrasion, low friction, and high insulation. Due to their versatility, DLC coatings have a broad range of applications across various industries. However, there is a need for further research on the hydrogen barrier functions of these coatings.

The combination of DLC coatings with buffer layers has been found to exhibit enhanced permeation resistance, particularly when applied to 316L stainless steel substrates [72]. The buffer layer comprises a two-tiered structure consisting of a metallic chromium coating, followed by a chromium nitride (CrN) layer, and finally topped with DLC. Notably, the synergy between the buffer layer and DLC coating, specifically when incorporating 20% hydrogen in the DLC, resulted in the lowest hydrogen permeation rate. A significant reduction of at least 1000-fold was observed compared to the permeation rate of the bare stainless steel substrate, demonstrating the effectiveness of this hybrid coating system in mitigating hydrogen permeation.

3.4.2. Graphene and Graphite. Recent research has focused on the potential of graphene to serve as a hydrogen barrier material, aimed at mitigating the embrittlement and oxidation of metals in industrial and nuclear reactor settings [73, 74]. Additionally, graphene has been explored as a means of hydrogen storage, typically involving high-pressure and low-temperature conditions [75].

According to a recent study [76], a composite coating comprising graphene oxide (GO) and aluminum oxide (Al_2O_3) was developed as a tritium permeation barrier through the sol-gel method. The resulting nanosheet-based composite exhibited a nine-fold increase in diffusion blocking efficiency (PRF = 9) compared to a pure Al_2O_3 coating at a temperature of 500 °C. Moreover, the toughness of the GO-Al_2O_3

composite coating was observed to have increased by 40%, suggesting enhanced mechanical robustness and potential applications in high-temperature environments.

The effects of neutron irradiation on hydrogen retention in graphite were investigated and found that the amount of retained hydrogen increased by a factor of 100 [77]. The results suggest that neutron irradiation can create hydrogen trapping sites, thereby reducing the diffusivity of hydrogen.

3.4.3. Carbides. A considerable body of research has focused on the utilization of carbides as hydrogen permeation barriers, with titanium carbide (TiC) and silicon carbide (SiC) being two of the most extensively studied materials. However, the deposition of TiC via CVD is a challenging process. To overcome this limitation, a composite material composed of TiC and titanium nitride (TiN) has been developed, which exhibits a significantly enhanced hydrogen permeation rate factor, approximately 10 times higher than that of TiC alone [78].

Silicon carbide (SiC), commonly referred to as Carborundum, has emerged as a promising material for the development of advanced fuel claddings to replace traditional zirconium-based alternatives. This is due to its notable advantages, including a significantly higher melting point, enhanced corrosion resistance at elevated temperatures, and comparable thermal neutron capture cross-sections to zirconium.

SiC coatings exhibit exceptional hardness, thermal conductivity, and oxidation resistance at elevated temperatures. Furthermore, SiC has been demonstrated to be an effective hydrogen permeation barrier. Notably, irradiation studies have been conducted to assess the material's stability, and results indicate that SiC retains its mechanical strength during Loss-of-Coolant Accident (LOCA) conditions up to at least 1300 °C [79].

Samples of 316 type of stainless steel (SS316) with a radio frequency (RF) sputtered SiC coating showed an order of magnitude reduction in hydrogen permeation at temperatures above 500 °C [80].

According to the research presented in [81], a temperature-dependent phenomenon was observed in silicon carbide, wherein the irradiation of the material at 300 °C resulted in a significant enrichment of carbon near grain boundaries (GBs). This enrichment effect was found to diminish when the irradiation was conducted at a higher temperature of 600 °C. This radiation-induced segregation (RIS) phenomenon is a well-documented phenomenon that can occur in various metallic alloys, leading to significant changes in the microstructure and properties of these materials. The occurrence of RIS is often linked to the interaction between radiation and defects in the material, which can result in the preferential migration of impurities or solute atoms to specific regions, such as GBs, under irradiation.

A novel observation of segregation in silicon carbide has been made, wherein the phenomenon occurs at a significantly lower irradiation temperature compared to RIS in metals. The impact of carbon enrichment on hydrogen behavior in SiC remains unclear, but it is well established that hydride phases frequently precipitate at grain boundaries. In light of the potential application of SiC in nuclear reactors, it is essential to investigate this effect to mitigate potential hydrogen trapping or permeation enhancement effects.

The permeation flux of deuterium was quantified after subjecting silicon carbide fiber-reinforced SiC matrix ceramic composites to high-heat-flux neutron irradiation [82]. A comparative investigation was conducted on pristine SiC/SiC tubes and tubes coated with chromium nitride (CrN), chromium (Cr), and titanium nitride (TiN) via cathodic arc physical vapor deposition.

Hydrogen permeability in silicon carbide has been experimentally determined to be less than $1{\cdot}10^{-21}$ mol $H_2m^{-1}s^{-1}MPa^{-1/2}$ at a temperature of 250 °C [83]. Subsequent measurements of deuterium leak rates as a function of deuterium pressure at temperatures ranging from 300 to 500 °C revealed a correlation between the rate of permeation and the applied pressure. Specifically, a low heat flux resulted in deuterium leak rates as low as 10^{-11} atm-cc/s.

A higher heat flux was observed to induce deuterium leak rates spanning a range of 10^{-6} to 10^{-9} atm-cc/s. The Cr-coated SiC/SiC material exhibited significantly lower deuterium leak rates of 10^{-12} atm-cc/s at low heat flux conditions, with even lower values obtained for the CrN-coated SiC/SiC material.

3.5. MAX PHASES AND MXENES

MAX phases can also exhibit excellent hydrogen barrier properties, depending on the environment. These ternary ceramic compounds are composed of early transition metals (**M**) (Sc, Ti, V, Cr, Zr, Nb, Mo) combined with elements from the **A** group (mainly Al, Si, P, S, Ga, Ge, Pb) and carbon or nitrogen (**X**) [84]. Research has focused on several MAX phases as potential materials for hydrogen isotope barriers and nuclear cladding applications, including Ti_3AlC, Ti_3SiC_2, Ti_2AlC, and TiAlN.

In a study published in [85], the authors investigated the deuterium permeation behavior of Ti_2AlN coatings deposited on ferritic stainless-steel substrates. The researchers also examined the impact of pre-oxidation on the coating's performance, finding that the Ti_2AlN coating exhibited a PRF of 45 relative to stainless steel, while the pre-oxidized coating displayed a significantly enhanced PRF of 3700.

MXenes represent a novel class of two-dimensional layered materials, comprising carbides, nitrides, and carbonitrides [86]. The designation “MXene” originates from the process of extracting the “A” layer from MAX phases, with the suffix “-ene” appended due to the similarity to graphene. Currently, there exist approximately 150 MAX phases and 40 MXenes. The synthesis of MXenes involves the selective etching of a MAX phase. It is imperative to undertake a comprehensive investigation into the properties and performance of these materials as hydrogen barriers in order to better understand their efficacy in mitigating the permeation of hydrogen through various mediums.

4. FACTORS AFFECTING THE EFFECTIVENESS OF HYDROGEN PERMEATION

4.1. COMMON FACTORS FOR ALL TYPES OF COATINGS

The qualities of coatings are affected by factors including the crystalline structure of the material, the surface density, the difference of thermal expansion coefficients between the coating and the substrate, the coating thickness, and the coating preparation method.

4.1.1. Thermal Expansion Coefficient. It has been confirmed in the literature that austenitic and martensitic stainless steel like 16Mn and 316L steel has excellent hydrogen resistant ability [87] where 316L stainless steel is also used as the base material in most research. The thermal expansion coefficient is used as an index of adhesion. If the difference of the thermal expansion coefficients between the barrier and the stainless-steel substrate is too large, the coating on the surface of the steel may wrinkle and crack thereby forming holes as the temperature rises, bringing the hydrogen into direct contact with the substrate. Therefore, when selecting the adhesive layer, a material with good adhesion and close thermal expansion coefficient to the substrate should be chosen to keep the surface integrity of the HPB and to avoid the appearance of defects.

On the other hand, if the adhesion degree of the coating and the substrate is low, it may cause the coating to peel off the surface of the steel, and thus it is difficult to form a protective barrier layer. A subtle detachment of the film may lead to the accumulation of the hydrogen and trigger the crack. The adhesion degree of the coating and the substrate can be tested by a scratch test, acoustic emission, tangential friction, and electron probe techniques [88].

4.1.2. Thickness. Generally, the effect of hydrogen resistance increases along with the thickness of the coating. However, if the coating is too thick, it may cause cracking. For some two-dimensional materials, thin film can well prevent the hydrogen permeation. It was found that 0.2 μm of Er_2O_3 coating could reduce the deuterium permeation to about 1/10−1/20 [89].

4.1.3. Grain Size. As the coating layer captures hydrogen through grain boundaries, grain size and morphology play a particular role. Usually the smaller grain size, the smaller the grain boundary and the surface of the coating denser and, thus, the better the hydrogen resistance. For example, Al_2O_3 film consisting of fine crystal grains with diameters below 40 nm has found a superior hydrogen-permeation barrier effect. The microcrystalline structure with many grain boundaries is expected to provide effective hydrogen-barrier performance [90].

However, arguments remain that the microstructure rather than the particle size itself plays a more important role. Within the study on the relationship between deuterium permeation and the microstructure of yttrium oxide coating, it revealed that the permeation property of the coating is highly dependent on the microstructure [91]. The permeation did not depend so much on the grain size but rather on the pinholes and some cracks present on the surface of the coating. Moreover, high hydrogen permeability is expected if the grain has a columnar shape (>100 nm).

An overview of the hydrogen permeabilities for a variety of barrier coatings and for a selection of oxides, nitrides, carbides, metals and alloys is given in Fig. 18.

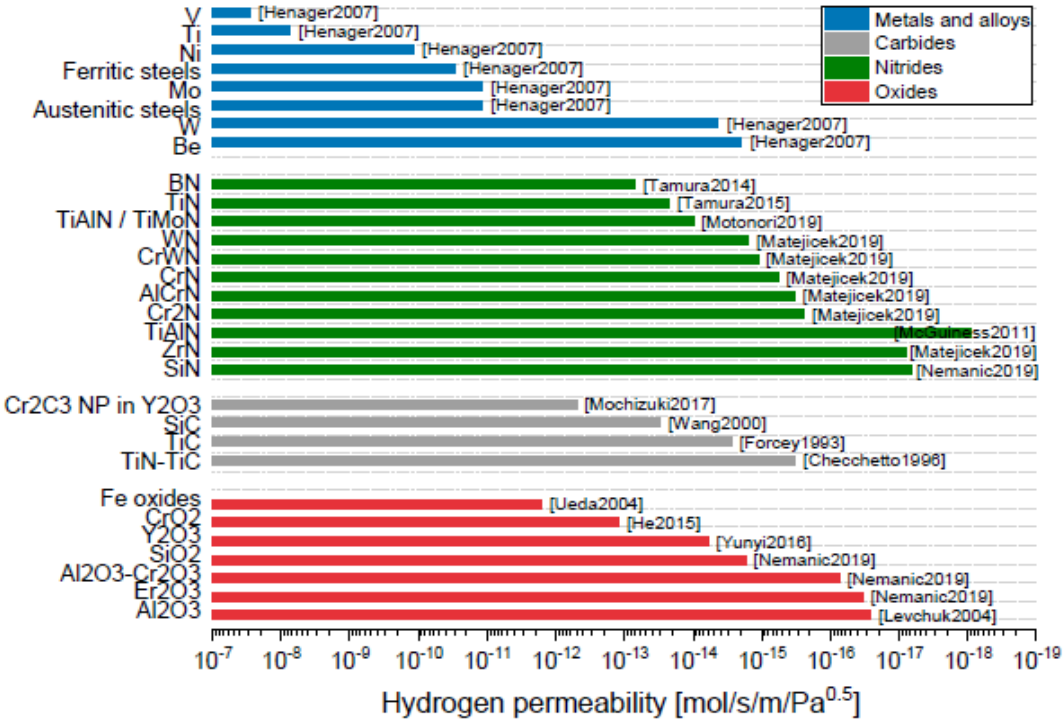

Fig. 18. The following table presents hydrogen permeabilities for state-of-the-art barrier coatings comprising various oxides, carbides, and nitrides, as reported in the literature. Additionally, permeabilities for a selection of metals and alloys are included for comparison purposes. The values provided are for a testing temperature range of 400 to 500°C, with extrapolated values where necessary [7]

4.1.4. Preparation Methods. Coating quality also varies against different preparation methods. For example, a SiC coating can be prepared either by ion beam-assisted deposition or ion implantation. Although high surface density coatings can be obtained with both methods, the hydrogen resistance efficiency of the coating prepared with the second method is higher [92]. Correctly developed complex approaches to creating coatings can provide exceptional barrier and anticorrosion effects even with a coating thickness of tens of nanometers. For instance, PVD coatings with additional oxidation of Cr_2O_3, CeO_2, YSZ, and Al_2O_3 on ferritic stainless steel (AISI 441) were exposed under dual-atmosphere conditions (Ar–5% H_2–3% H_2O) at 600 °C for up to 3000 h [93]. The best results were observed with 30 nm Al_2O_3 coatings, which drastically reduced dual-atmosphere corrosion and hydrogen effect.

There are different preparation techniques even for the same type of coating, which have both advantages and disadvantages. So, preparation methods must be chosen according to the various needs and situations. Special materials require special preparation methods, which need to be further combined with other technologies.

CONCLUSIONS

The performance of hydrogen permeation barriers is influenced by the choice of coating materials, their structure and preparation methods.

Metallic coatings are capable of forming metallurgical bonds with metallic substrates. However, their common columnar crystal structure has the adverse effect of reducing the permeability of the hydrogen barrier. The enhancement of hydrogen resistance in metal coatings necessitates microstructural modification, including the increase of the grain boundary density and the coating compactness. Future research should focus on the experimental investigation of the hydrogen resistance mechanisms of metallic coatings. Existing studies suggest that PVD is a promising method for producing dense metallic coatings.

Ceramic coatings, such as Al_2O_3 and Er_2O_3, exhibit low hydrogen permeability but face practical challenges, including poor adhesion to substrates, susceptibility to cracking and delamination, and stringent preparation conditions that hinder their industrial application. These challenges emphasize the need for innovative solutions that address the issues of adhesion, durability, and manufacturing feasibility in order to fully exploit the benefits of these ceramic coatings.

Nitride coatings, including TiN, CrN, ZrN, TiAlN, and their multilayer combinations, are known to exhibit high wear resistance, adhesion, and crack resistance compared to oxide coatings. These coatings also demonstrate high barrier properties against hydrogen, meeting the industrial requirements for such coatings.

Two-dimensional materials such as graphene, MXene, and other nanosheets offer significant potential for improving hydrogen barrier performance by extending hydrogen permeation paths and blocking defects in adjacent nanosheets. However, the fabrication of graphene coatings on complex structures, particularly on the inner walls of pipelines by CVD, remains a challenge.

Composite hydrogen permeation barriers that combine multiple components are gaining attention due to their superior properties, including improved hydrogen permeability, bonding strength, and surface morphology. These materials are typically prepared by doping, mixing different materials, or layer-by-layer techniques. Improvement methods such as increasing grain boundaries, introducing transition layers to improve coating-substrate bonding, exploiting the template effect, and forming interfacial hydrogen traps are promising. Future developments may include coatings with a "hydrogen barrier – hydrogen storage" composite structure, trapping hydrogen atoms that pass through the barrier layer.

The quality of the coating is influenced by a number of factors, including the selection of coating materials, surface preparation, deposition conditions (process temperature, particle energy, deposition rate, gas pressure, etc.), good adhesion, crystalline (fine grain, texture, etc.) or amorphous structure, absence of open porosity, and deposition methods.

In summary, advances in HPB preparation technology are critical for both scientific research and commercial applications. From an industrial perspective, improving preparation efficiency and reducing associated costs are essential to meet the demands of large-scale production.

ACKNOWLEDGEMENTS

The work was financially supported by the National Academy of Science of Ukraine (program "Support of the development of main lines of scientific investigations" (KPKVK 6541230)).

REFERENCES

1. S.J. Kim, K.Y. Kim. An Overview on Hydrogen Uptake, Diffusion and Transport Behavior of Ferritic Steel, and Its Susceptibility to Hydrogen Degradation // *Corros. Sci. Technol*. 2017, v. 16, p. 209-225.
2. S.A. Karpov, G.D. Tolstolutskaya, V.N. Voyevodin. The most probable mechanisms of material characteristics degradation due to accumulation of hydrogen and predicting the possible scenarios of maintain its resource // *PAST*. 2018, N 5(117), p. 3-15.
3. M. Koyama; E. Akiyama, Y.-K. Lee, D. Raabe, K. Tsuzaki. Overview of Hydrogen Embrittlement in High-Mn Steels // *Int. J. Hydrog. Energy*. 2017, v. 42, p. 12706-12723.
4. J. Song, W.A. Curtin. Atomic Mechanism and Prediction of Hydrogen Embrittlement in Iron // *Nat. Mater.* 2013, v. 12 (2), p. 145-151.
5. J. Yamabe, S. Matsuoka, Y. Murakami. Surface coating with a high resistance to hydrogen entry under high-pressure hydrogen-gas environment // *Int. J. Hydrog. Energy*. 2013, v. 38. p. 10141-10154.
6. L. Liu, Q. Ruan, S. Xiao, X. Meng, et al. Fabrication and hydrogen permeation resistance of dense CrN coatings // *Surf. Coat. Technol*. 2022, v. 437, p. 128326.
7. M. Wetegrove, M.J. Duarte, A. Taube. Preventing Hydrogen Embrittlement: The Role of

Barrier Coatings for the Hydrogen Economy // *Hydrogen*. 2023, v. 4, p. 307-322.

8. J. Serp, M. Allibert, O. Benes, et al. The molten salt reactor (MSR) in generation IV: Overview and perspectives // *Prog. Nucl. Energy*. 2014, v. 77, p. 308-319.

9. Ewa C. E. Rönnebro, Robert L. Oelrich, and Robert O. Gates. Recent Advances and Prospects in Design of Hydrogen Permeation Barrier Materials for Energy Applications–A Review // *Molecules*. 2022, v. 27(19), p. 6528.

10. *Gaseous hydrogen embrittlement of materials in energy technologies*. V. 2: *Mechanisms, modelling and future developments* / Edited by Richard P. Gangloff and Brian P. Somerday. Woodhead Publishing Limited, 2012, 500 p.

11. P.V. Geld, R.A. Ryabov, E.S. Kodes. *Hydrogen and imperfections in the structure of metals.* M.: "Metallurgy", 1979, 221 p.

12. Z. Yao, C. Liu, and P. Jung. Diffusion and Permeation of Deuterium in EUROFER97: Effect of Irradiation and of Implanted Helium // *Fusion Sci. Technol*. 2005, v. 48, p. 1285-1291.

13. S. Karpov, V. Ruzhits'ky, I. Neklyudov, V. Bendikov, G. Tolstoluts'ka. Parameters of trapping and the thermoactivated output of the deuterium ion-implanted into the Cr18Ni10Ti steel // *Metallofiz. Noveish. Tekhnol*. 2004, v. 26, #12, p. 1661-1670 (in Russian).

14. K. Ono, M. Miyamoto, K. Arakawa, S. Matsumoto, F. Kudo. Effects of precipitated helium, deuterium or alloy elements on glissile motion of dislocation loops in Fe-9Cr-2W ferritic alloy // *J. Nucl. Mater*. 2014, v. 455, N 1-3, p. 162-166.

15. S.M. Myers, P. Nordlander, F. Besenbacher, et al. Theoretical examination of the trapping of ion implanted hydrogen in metals // *Phys. Rev. B.* 1986, v. 33, N 2, p. 854-863.

16. A. Atrens, N.F. Fiore, K. Miura. Dislocation damping and hydrogen pinning in austenitic stainless steels // *J. Appl. Phys.* 1977, v. 48, N 10, p. 4247-4251.

17. S.A. Karpov, G.D. Tolstolutskaya, B.S. Sungurov, V.V. Ruzhytskiy. Microstructure evolution and deuterium trapping in low-energy cascades after irradiation of SS316 stainless steel // *PAST*. 2017, N 2(108), p. 36-40.

18. D. Perez Escobar, E. Wallaert, L. Duprez, A. Atrens, K. Verbeken. Thermal desorption spectroscopy study of the interaction of hydrogen with TiC precipitates // *Met. Mater. Int*. 2013, v. 19, p. 741-748.

19. D. Perez Escobar, L. Duprez, A. Atrens, K. Verbeken. Influence of experimental parameters on thermal desorption spectroscopy measurements during evaluation of hydrogen trapping // *J. Nucl. Mater*. 2014, v. 450, p. 32-41.

20. M. Beghini, G. Benamati, et al. Effect of hydrogen on the ductility reduction of F82H martensitic steel after different heat treatments // *J. of Nucl. Mater*. 2001, v. 288, p. 1-6.

21. V. Nemanič. Hydrogen permeation barriers: Basic requirements, materials selection, deposition methods, and quality evaluation // *Nucl. Mater. Energy*. 2019, v. 19, p. 451-457.

22. F.-W. Bach, K. Möhwald, A. Laarmann, T. Wenz. *Moderne Beschichtungsverfahren*. John Wiley & Sons: Hoboken, NJ, USA, 2006.

23. H. Lei, H. Di, J. Lijun, L. Xiaopeng, Y Quinghe. L. Shuai, D. Miao. *$Y_2O_3/Al_2O_3/Cr_2O_3$ Composite Gradient Hydrogen Resistant Coating and Preparation Method.* Thereof. China Patent CN105667009A, 26 December 2014.

24. C. Henager. *Hydrogen Permeation Barrier Coatings // In Materials for the Hydrogen Economy.* CRC Press: Boca Raton, FL, USA, 2007, Chapter 8, p. 181-190.

25. J. Harhausen, R. Brinkmann, R. Foest, M. Hannemann, A. Ohl, B. Schröder. On plasma ion beam formation in the Advanced Plasma Source // *Plasma Sources Sci. Technol*. 2012, v. 21, p. 035012.

26. Y. Yamada-Takamura, F. Koch, H. Maier, H. Bolt. Hydrogen permeation barrier performance characterization of vapor deposited amorphous aluminum oxide films using coloration of tungsten oxide // *Surf. Coat. Technol*. 2002, v. 153, p. 114-118.

27. A.S. Kuprin, R.L. Vasilenko, G.D. Tolstolutskaya, V.N. Voyevodin, et al. Irradiation resistance of chromium coatings for ATFC in the temperature range 300-550 °C // *J. of Nucl. Mater*. 2021, v. 549, p. 152908.

28. A.S. Kuprin, V.A. Belous, V.N. Voyevodin, et. al. Irradiation resistance of vacuum arc chromium coatings for zirconium alloy fuel claddings // *J. of Nucl. Mater*. 2018, v. 510, p.163-167.

29. R. Frauenfelder. Solution and diffusion of hydrogen in tungsten // *J. Vac. Sci. Technol*. 1969, v. 6, p. 388-395.

30. B. Zajec. Hydrogen permeation barrier – recognition of defective barrier film from transient permeation rate // *Int. J. Hydrog. Energy*. 2011, v. 36, p. 7353-7361.

31 A.S. Kuprin, V.A. Zuyok, V.A. Belous, et al. Protective vacuum-arc coatings on zirconium alloy fuel cladding to prevent catastrophic accidents at nuclear reactors // *PAST*. 2023, N 2(144), p. 94-104.

32. M. Sevecek, A. Gurgen, A. Seshadri, et al. Development of Cr cold spray-coated fuel cladding with enhanced accident tolerance // *Nucl. Eng. Technol*. 2018, v. 50, p. 229-236.

33. K.G. Field, M.A. Snead, Y. Yamamoto, K.A. Terrani. *Handbook on the Material Properties of FeCrAl Alloys for Nuclear Power Production Applications* / U.S. Department of Energy Office of Scientific and Technical Information; Oak Ridge, TN, USA, 2018. ORNL/TM-2018/905.

34. G.D. Tolstolutska, V.V. Ruzhytskyi, I.E. Kopanets, O.S. Kuprin et al. Specific features of saturation with deuterium of vacuum-arc coatings based on iron // *Materials Science.* 2020, v. 56, N 1, p. 34-42.

35. A. Gilewicz, P. Chmielewska, D. Murzynski, E. Dobruchowska, B. Warcholinski. Corrosion resistance of CrN and CrCN/CrN coatings deposited using cathodic arc evaporation in Ringer's and Hank's solutions // *Surface and Coatings Technology.* 2016, v. 299, p. 7-14.

36. K. Daub, R. van Nieuwenhove, H. Nordin. Investigation of the impact of coatings on corrosion and

hydrogen uptake of Zircaloy-4 // *J. Nucl. Mater.* 2015, v. 467, p. 260-270.

37. S. Fite, I. Zukerman, A. Ben Shabat, S. Barzilai. Hydrogen protection using CrN coatings: Experimental and theoretical study // *Surfaces and Interfaces*. 2023, v. 37, p. 102629.

38. D. Shin, S. Kim. Effect of hydrogen charging on the mechanical characteristics and coating layer of CrN-coated aluminum alloy for light-weight FCEVs // *Japanese Journal of Applied Physics*. 2023, v. 62, SN1004.

39. I.E. Kopanetz, G.D. Tolstolutskaya, A.V. Nikitin, et al. The effect of Cr, Cr-N and Cr-O_x coatings on deuterium retention and penetration in zirconium alloy Zr-1Nb // *PAST.* 2015, N 5, p. 81-86.

40. M. Tamura. Hydrogen Permeation Characteristics of TiN-Coated Stainless Steels // *J. Mater. Sci. Eng*. 2015, v. A5, p. 197-201.

41. M. Tamura, T. Eguchi. Nanostructured thin films for hydrogen-permeation barrier // *J. Vac. Sci. Technol. A Vac. Surf. Films.* 2015, v. 33, p. 041503.

42. E. Alat, A.T. Motta, R.J. Comstock, J.M. Partezana, D.E. Wolfe. Multilayer (TiN, TiAlN) ceramic coatings for nuclear fuel cladding // *J. Nucl. Mater.* 2016, v. 478, p. 236-244.

43. M. Tamura, H. Takizawa. TiAlN/TiMoN Coatings as Hydrogen Barriers // *Journal of Materials Science and Engineering*. 2019, v. A 9 (1-2), p. 1-7.

44. J. Matějíčeka, J. Veverkaa, V. Nemanič. Characterization of less common nitrides as potential permeation barriers // *Fusion Eng. Des*. 2019, v. 139, p. 74-80.

45. Kuan-Che Lan, Yan-Ting Chen, Hsiao-Ming Tung, Yi-Fan Tseng, Yu-Chen Li. Hydrogen permeation resistance of ZrN thin film deposited by ion-plating // *Surface and Coatings Technology*. 2024, v. 484, p. 130866.

46. J. Roth, E. Tsitrone, T. Loarer, et al. Tritium inventory in ITER plasma-facing materials and tritium removal procedures // *Plasma Phys. Control Fusion*. 2008, v. 50, p. 103001.

47. J. Roth, K. Schmid. Hydrogen in tungsten as plasma-facing material // *Phys. Scripta*. 2011, v. T145, p. 014031.

48. G.D. Tolstolutskaya, A.S. Kuprin, A.V. Nikitin, et al. Deuterium trapping and sputtering of tungsten coatings exposed to low-energy deuterium plasma // *PAST.* 2020, N 2(126), p. 54-59.

49. I.I. Aksenov, A.A. Andreev, V.A. Belous, V.E. Strel'nitskij, V.M. Khoroshikh. *Vacuum arc: plasma sources, deposition of coatings, surface modification.* Kiev: "Naukova Dumka", 2012.

50. O.V. Ogorodnikova. Fundamental aspects of deuterium retention in tungsten at high flux plasma exposure // *Journal of Applied Physics*. 2015, v. 118, p. 074902.

51. A. Houben, M. Rasiński, L. Gao, C. Linsmeier. Tungsten nitride as tritium permeation barrier // *Nucl. Mater. Energy.* 2020, v. 24, p. 100752.

52. P. Díaz-Rodríguez, M. Panizo-Laiz, C. González, et al. Direct observation of hydrogen permeation through grain boundaries in tungsten // *Emerg. Mater.* 2022, v. 5, p. 1075-1087.

53. R. van Nieuwenhove, V. Andersson, J. Balak, B. Oberlander. In-Pile Testing of CrN, TiAlN and AlCrN Coatings on Zircaloy Cladding in the Halden Reactor, Zirconium in the Nuclear Industry // *18th International Symposium, STP 1597. ASTM International*; West Conshohocken, PA, USA, 2016, p. 965-982.

54. I. Levin, D. Brandon. Metastable Alumina Polymorphs: Crystal Structures and Transition Sequences // *J. Am. Ceram. Soc.* 1998, v. 81, p. 1995-2012.

55. G.W. Hollenberg, E.P. Simonen, G. Kalinin. Tritium/hydrogen barrier development // *Fusion Eng. Des*. 1995, v. 28, p. 190-208.

56. D. Iadicicco, S. Bassini, M. Vanazzi, et al. Efficient hydrogen and deuterium permeation reduction in Al_2O_3 coatings with enhanced radiation tolerance and corrosion resistance // *Nucl. Fusion*. 2018, v. 58, p. 126007.

57. R.A. Youngman, T.E. Mitchell, F.W. Clinard, G.F. Hurley. High dose neutron irradiation damage in alpha alumina // *J. Mater. Res*. 1991, v. 6, p. 2178-2187.

58. G.P. Pells. Radiation Damage Effects in Alumina // *J. Am. Ceram. Soc*. 1994, v. 77, p. 368-377.

59. A. Morono, E.R. Hodgson, M. Malo. Radiation enhanced deuterium absorption for Al_2O_3 and macor ceramic // *Fusion Eng. Des.* 2013, v. 88, p. 2488-2491.

60. F.G. Ferré, A. Mairov, L. Ceseracciu, et al. Radiation endurance in Al_2O_3 nanoceramics // *Sci. Rep*. 2016, v. 6, p. 33478.

61. A. Couet, A.T. Motta, R.J. Comstock. Hydrogen pickup measurements in zirconium alloys: Relation to oxidation kinetics // *J. Nucl. Mater*. 2014, v. 451, p. 1-13.

62. K. Hashizume, K. Ogata, S. Akamaru, Y. Hatano. Solubility of hydrogen isotopes in zirconia ceramics // *J. Plasma Fusion Res. Ser.* 2013, v. 10, p. 33-35.

63. M. Youssef, M. Yang, B. Yildiz. Doping in the Valley of Hydrogen Solubility: A Route to Designing Hydrogen-Resistant Zirconium Alloys // *Phys. Rev. Appl.* 2016, v. 5, p. 014008.

64. Y. Hatano, K. Zhang, K. Hashizume. Fabrication of ZrO_2 coatings on ferritic steel by wet-chemical methods as a tritium permeation barrier // *Phys. Scr.* 2011, v. 2011, #T145, p. 014044.

65. X. Xiang, X. Wang, G. Zhang, T. Tang, X. Lai. Preparation technique and alloying effect of aluminide coatings as tritium permeation barriers: A review // *Int. J. Hydrog. Energy*. 2015, v. 40, p. 3697-3707.

66. F. Yang, X. Xiang, G. Lu, et al. Tritium permeation characterization of Al_2O_3/FeAl coatings as tritium permeation barriers on 321 type stainless steel containers // *J. Nucl. Mater.* 2016, v. 478, p. 144-148.

67. X. Xiang, F. Yang, G. Zhang, X. Wang. Effect of Steel Substrates on the Formation and Deuterium Permeation Resistance of Aluminide Coatings // *Coatings*. 2019, v. 9, p. 95-108.

68. U. Prakash, N. Parvathavarthini, R.K. Dayal. Effect of composition on hydrogen permeation in Fe-Al alloys // *Intermetallics.* 2007, v. 15, p. 17-19.

69. Z. Xin, X. Yin, Y. Ling et al. Hydrogen permeation behavior and mechanism of Cr_2O_3/Al_2O_3 bipolar oxide film under plasma discharging

environment // *Int. J. Hydrogen Energy*. 2017, v. 42, p. 20869-20878.

70. Q. Li, J. Wang, Q.Y. Xiang, et al. Novel nano-crystalline Er_2O_3 hydrogen isotopes permeation barriers // *J. Eur. Ceram. Soc.* 2017, v. 37, p. 249-254.

71. W. Mao, M. Wilde, T. Chikada, et al. Fabrication and Hydrogen Permeation Properties of Epitaxial Er_2O_3 Films Revealed by Nuclear Reaction Analysis // *J. Phys. Chem. C*. 2016, v. 120, p. 15147-15152.

72. M. Tamura, T. Kumagai. Hydrogen permeability of diamondlike amorphous carbons // *J. Vac. Sci. Technol*. 2017, v. 35, p. 04D101-04D108.

73. Y. Fan, Y. Huang, B. Cui, Q. Zhou. Graphene coating on nickel as effective barriers against hydrogen embrittlement // *Surf. Coat. Technol.* 2019, v. 374, p. 610-616.

74. A.A. Sagade, A.I. Aria, S. Edge et al. Graphene-based nanolaminates as ultra-high permeation barriers // *Npj 2D Mater. and Appl.* 2017, v. 1, p. 35-43.

75. V. Tozzini, V. Pellegrini. Prospects for hydrogen storage in graphene // *Phys. Chem. Chem. Phys*. 2013, v. 15, p. 80-89.

76. Y. Su, V.G. Kravets, S.L. Wong, et al. Impermeable barrier films and protective coatings based on reduced graphene oxide // *Nat. Commun*. 2014, v. 5, p. 4843-4848.

77. H. Atsumi, N. Shibata, T. Tanabe, T. Shikama. Hydrogen absorption into neutron-irradiated graphite and estimation of the trapping effect // *Phys. Scr.* 2007, v. T128, p. 72-75.

78. V. Nemanič. Hydrogen permeation barriers: Basic requirements, materials selection, deposition methods, and quality evaluation // *Nucl. Mater. Energy*. 2019, v. 19, p. 451-457.

79. K. Barrett, S. Bragg-Sitton, D. Galicki. *Advanced LWR Nuclear Fuel Cladding System Development Trade-off Study.* Idaho National Laboratory. INL/EXT-12-27090: Idaho National Laboratory Light Water Reactor Sustainability Program, 2012.

80. T. Usui, A. Sawada, M. Amaya, A. Suzuki, T. Chikada, T. Terai. SiC coating as hydrogen permeation reduction and oxidation resistance for nuclear fuel cladding // *Journal of Nuclear Science and Technology*. 2015, v. 52 (10), p. 1318-1322.

81. X. Wang, H. Zhang, T. Baba et al. Radiation-induced segregation in a ceramic // *Nat. Mater*. 2020, v. 19, p. 992-998.

82. X. Hu, T. Koyanagi, Y. Katoh. Report on Hydrogen Isotope Permeability/Hermeticity of SiC-Based Cladding. Oak Ridge National Lab. (ORNL); Oak Ridge, TN, USA: 2019. ORNL/TM-2019/1187.

83. R.A. Causey, W.R. Wampler, J.R. Retelle, J.L. Kaae. Tritium migration in vapor-deposited beta-silicon carbide // *J. Nucl. Mater.* 1993, v. 203, p. 196-205.

84. M. Sokol, V. Natu, S. Kota, M.W. Barsoum. On the Chemical Diversity of the MAX Phases // *Trends Chem*. 2019, v. 1, p. 210-223.

85. L. Gröner, L. Mengis, M. Galetz, L. Kirste. P. Daum. Investigations of the Deuterium Permeability of As-Deposited and Oxidized Ti_2AlN Coatings // *Materials.* 2020, v. 13, p. 2085-2093.

86. K. Shi, X. Meng, S. Xiao, et al. MXene Coatings: Novel Hydrogen Permeation Barriers for Pipe Steels // *Nanomaterials.* 2021, v. 11, p. 2737-2747.

87. J. Zhai, T. Xu, H. Wang, G. Ma, X. Shang. The High Pressure Hydrogen Embrittlement Research of 316L and 16Mn // *Materials Reports.* 2019, v. 33, p. 497-500.

88. W. Ding, C. Qian, Y. Chen, C. Wang, F. Meng. Methods of Measurement and Evaluation of Adhesion Force between Film and Base Body // *Modern vehicle power*. 2014, v. 4, p. 55-58.

89. Q. Li, J. Wang, Q.-Y. Xiang, T. Tang, Y.-C. Rao, J.-L. Cao. Thickness Impacts on Permeation Reduction Factor of Er_2O_3 Hydrogen Isotopes Permeation Barriers Prepared by Magnetron Sputtering // *Int. J. Hydrogen Energy*. 2016, v. 41 (4), p. 3299-3306.

90. Y. Wu, D. He, S. Li, X. Liu, S. Wang, L. Jiang. Deuterium Permeation Properties of Y_2O_3/Cr_2O_3 Composite Coating Prepared by MOCVD on 316L Stainless Steel // *Int. J. Hydrogen Energy.* 2016, v. 41(18), p. 7425-7430.

91. Y. Wu, D. He, S. Li, X. Liu, S. Wang, L. Jiang. Microstructure Change and Deuterium Permeation Behavior of the Yttrium Oxide Coating Prepared by MOCVD // *Int. J. Hydrogen Energy.* 2014, v. 39(35), p. 20305-20312.

92. P. Wang, J. Liu, Y. Wang, B. Shi. Investigation of SiC Films Deposited onto Stainless Steel and their Retarding Effects on Tritium Permeation // *Surf. Coat. Technol.* 2000, v. 128-129 (1), p. 99-104.

93. M. Tomas, J.-E. Svensson, J. Froitzheim. Hydrogen-barrier coatings against dual-atmosphere corrosion for IT-SOFC interconnect applications // *Int. J. Hydrogen Energy*. 2024, v. 58(8), p. 852-862.

Article received 26.06.2024

БАР'ЄРНІ ПОКРИТТЯ ДЛЯ ВОДНЮ ТА ЇХ СТІЙКІСТЬ ДО ПРОНИКНЕННЯ

Г.Д. Толстолуцька, М.О. Азарєнков, В.А. Білоус, О.С. Купрін, М.Г. Іщенко

Обговорюється сучасний стан досліджень проникнення водню у різні покриття. Потрапляння водню у конструкційні матеріали може бути шкідливим через корозію і крихкість. Щоб уможливити безпечну експлуатацію в умовах, що вимагають захисту від ізотопів водню, узагальнено останні досягнення у дизайні матеріалів і характеристиках бар'єрних покриттів, які запобігають проникненню і поглинанню ізотопів водню. Альтернативні концепції покриттів можуть забезпечити більшу стійкість до проникнення ізотопів водню разом з іншими покращеними властивостями, такими як механічна міцність і термостійкість. Представлена тут інформація зосереджена на нещодавніх дослідженнях перспективних водневих бар'єрів, включаючи оксиди, нітриди, вуглець, карбіди, MAX-фази і метали, а також їх механічну міцність, поглинання водню і радіаційну стійкість.